MULTISCALE DAMAGE MODELLING WITH A "MORPHOLOGICAL APPROACH" TO HIGHLIGHT PARTICLE SIZE EFFECT IN HIGHLY-FILLED PARTICULATE COMPOSITES

M. Trombini[a*], C. Nadot-Martin[a], D. Halm[a], G. Contesse[b], A. Fanget[b]

[a]*Département de Physique et Mécanique des Matériaux, Institut Pprime – CNRS – ENSMA – Université de Poitiers, UPR 3346, Futuroscope Chasseneuil Cedex, France*
[b]*Commissariat à l'Energie Atomique et aux Energies Alternatives, Centre d'Etudes de Gramat, Gramat, France*
**marion.trombini@ensma.fr*

Keywords: propellants, multiscale modeling, particle size effect, interface debonding.

Abstract
A multiscale modeling specially adapted to highly-filled particulate composites is introduced. This approach, the "Morphological Approach", allows a direct solving in spite of the material non-linearities. Under a mechanical loading, the global and local responses are estimated. In this framework, particle size effects expected into this type of materials are studied. Considering the constituents (particles and matrix) as linear elastic, numerical computations are performed on simple periodic cells, random monomodal microstructures and random bimodal microstructure. Particle / matrix debonding chronology is evaluated, considering the size of particles and also interaction between particles.

1. Introduction

This work focuses on the mechanical behavior of highly-filled particulate composites, such as propellant-like materials, which are characterized by an elastomeric matrix and a high volume fraction of reactive particles (greater than 60%). Due to its composition, this type of materials is really concerned with regard to its vulnerability [1]. Damage by interfacial debonding between particles and the binder is a well-known phenomenon in highly-filled particulate composites. The complex morphology and the strongly non-linear behavior of propellant materials (finite strains, interfacial damage, etc.) led to the progressive development of a specific multiscale technique which enables the access to local fields and to the homogenized response. This method, the "Morphological Approach" (M.A.), allows the explicit geometrical representation of the whole microstructure (particles, intergranular zones, spatial distribution). A simplified kinematical framework allows a direct solving, without any prior linearization of local non-linear constitutive laws [2]. It avoids concerns about the choice of a linearization method. This approach gives the access to local field estimations with the description of heterogeneity into the matrix depending on local morphology. The modeling of the evolution of interfacial damage through particle/matrix debonding leads to the characteristics of defects in the microstructure and induced effects at different scales [3].
This paper deals with the M.A. as proposed in [3], that is considering linear elastic constituents and interfacial damage evolution. We try to evaluate its predictive capacities regarding particle size effects and interaction between particles. Particle size really influences

the energetic and mechanical behavior of energetic composites [4,5], and plays an important role in damage phenomenology. It is experimentally observed that, under quasi-static loadings, interface debondings occur preferentially on large particles into highly-filled particulate composites [6]. Moreover, interfacial debonding is observed preferentially in areas where the particle volume fraction is higher, that is when interaction between particles is more important [7]. Consequently, we try to observe these effects on different types of microstructures with the M.A., through numerical simulations. We consider the following cases: unit cells, random monomodal and bimodal microstructures numerically generated.

2. The Morphological Approach in the small strain framework with evolutive damage

2.1. Microstructure representation and main hypotheses

The considered microstructure is constituted of an aggregate of grains in high volume fraction and randomly distributed. It is represented through a numerical process by polyhedral grains interconnected by thin matrix layers with uniform thicknesses [2,3,8]. The interfaces of opposite polyhedra are parallel. Considering the microstructure in its initial and non-deformed configuration, four morphological parameters are identified for a layer α: the thickness of the layer h^α, the projected area A^α, the vector $\mathbf{d}^\alpha$ linking the centroids of the polyhedra which are on both sides of the layer and the unit normal vector $\mathbf{n}^\alpha$ defining the orientation of the grain/layer reference interface (Figure 1).
A simplified kinematical description is associated to this morphological representation, through four hypotheses [3]. In this way, while (i) the centroids of the grains have a global motion defined by the macroscopic displacement gradient **F** (data for the problem), (ii) the grains are supposed to be subjected to a homogeneous displacement gradient $\mathbf{f}^0$ which is identical for all grains. (iii) Each layer α is subjected to a homogeneous displacement gradient $\mathbf{f}^\alpha$ which can be different from one layer to another. Finally, (iv) local disturbances at grain edges and corners are neglected.

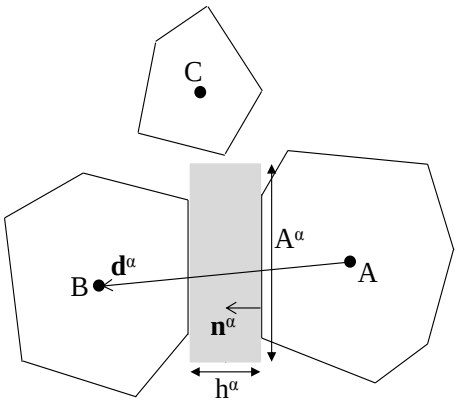

Figure 1. Morphological parameters characterizing a layer α.

2.2. Interfacial debonding and evolutive damage in the small strain framework

Interfacial defects have been incorporated in a compatible way with the M.A. kinematical hypotheses [9]. Relative displacement jumps across the interfaces have been defined, characterizing defects, while considering a continuous displacement field across the sound interfaces. Kinematical hypotheses described in 2.1 impose that displacement discontinuity vector across the debonded interface is an affine function of spatial coordinates. We consider

two configurations allowed by the assumption of a homogeneous displacement gradient for each grain: either no debonding or simultaneous debonding of both interfaces.
Conditions written at the interfaces lead to the expression of the displacement gradient of a layer α. It depends on the displacement gradient of the grains $\mathbf{f}^0$, the macroscopic displacement gradient **F**, the morphological data and an additional term called $\mathbf{f}^{\alpha D}$ [9]:

$$f_{ij}^{\alpha} = f_{ij}^{0} + (F - f^{0})_{ik} \frac{d_k^{\alpha} n_j^{\alpha}}{h^{\alpha}} + f_{ij}^{\alpha D} \tag{1}$$

The latter term represents the specific contribution of the pair of defects at the interfaces of the debonded layer α. If the layer is sound (without interfacial defects), the term $\mathbf{f}^{\alpha D}$ does not exist.
The compatibility between the local and the global motions (described by the data of the displacement gradient **F**) is ensured through the following condition to be satisfied by morphological parameters:

$$\frac{1}{|V|} \sum_{\alpha} d_i^{\alpha} n_j^{\alpha} A^{\alpha} = \delta_{ij} \tag{2}$$

where δ_{ij} is the Kronecker symbol and $|V|$ is the volume of the schematized microstructure.
The generalized Hill lemma taking into account discontinuities across interfaces associated to homogeneous stress boundary conditions gives:

$$(1-c)\sigma_{ij}^{0} + \frac{1}{|V|} \sum_{\alpha} \sigma_{ij}^{\alpha} A^{\alpha} h^{\alpha} - \frac{1}{|V|} \sum_{\alpha} t_i^{\alpha} d_j^{\alpha} = 0 \tag{3}$$

where $c = \frac{1}{|V|} \sum_{\alpha} A^{\alpha} h^{\alpha}$ is the matrix volume fraction and $t_i^{\alpha} = \sigma_{ik}^{\alpha} n_k^{\alpha} A^{\alpha}$ is the total force transmitted through the layer α. $\boldsymbol{\sigma}^0$ is the average stress tensor over the volume of the grains and $\boldsymbol{\sigma}^{\alpha}$ is the average stress tensor over the volume of a layer α.
The introduction of local constitutive laws in equation (3) – linear elastic for this study [3] – combined to equations (1) and (2), gives an equation in which the displacement gradient of the grains $\mathbf{f}^0$ is the main unknown quantity. The expression of $\mathbf{f}^0$ is obtained as a function of **F** and $\mathbf{f}^{\alpha D}$ through an analytical solving of this equation. With $\mathbf{f}^0$ and equation (1), we deduce the displacement gradients $\{\mathbf{f}^{\alpha}\}$ for every layer, local strains, Cauchy stresses, and then homogenized stress. The quantities $\{\mathbf{f}^{\alpha D}\}$, induced by interfacial defects, depend on the imposed macroscopic loading. Their expression has been determined through complementary homogenization-localization procedures [3,9].
Here, we only consider open interfacial defects (called α = β) and nucleation. Dartois et al. [3] also considered closed interfacial defects (called f), closure and re-opening of defects.
Nucleation of interfacial defects is supposed to happen in opening mode. This hypothesis leads to a specific nucleation criterion defining interfacial debonding [3]. For that purpose, two points P_1 and P_2 are located on each side of the reference interface $I^{1\alpha}$ of every undamaged layer α (Figure 2), respectively in the grain and in the matrix. These two points are each at the same distance λ from their normal projection B_1 on the interface. B_1 is the gravity center of $I^{1\alpha}$. To set the nucleation criterion, the normal projection d_{norm}^{α} of the difference of actual positions of P_1 and P_2 on the normal $\mathbf{n}^{\alpha}$ is expressed. Debonding happens

on both interfaces of the layer α as soon as this distance d^{α}_{nom} reaches a certain critical value d_{crit}.

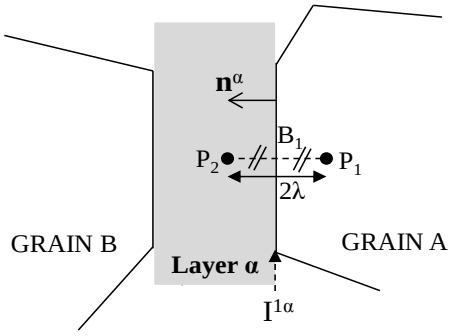

Figure 2. Schematization and parameters to define interfacial debonding.

3. Particle size effect and interaction effects on debonding chronology

The M.A. is evaluated through numerical simulations on various microstructures. We approach this study with growing difficulties. First, periodic cells are considered, then random monomodal microstructures and finally random bimodal microstructure.

3.1. Evaluation on periodic cells

We consider a simple cell constituted of a cubic particle of dimension L and three layers of matrix disposed on three adjacent facets of this grain (Figure 3). A periodic microstructure can be built thanks to the repetition of this cell with simple translations. Constituents have a linear elastic behavior [3].

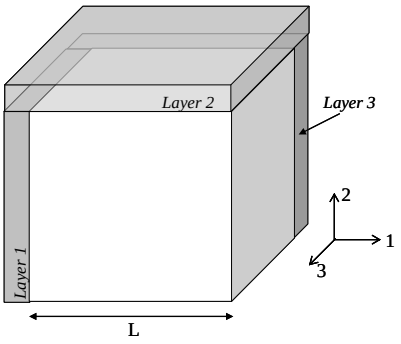

Figure 3. Periodic cell.

3.1.1. Particle size effect

In order to study particle size effect for these periodic cells, we consider different unit cells with the same matrix volume fraction and the same damage parameters (d_{crit}, λ). Only the particle size changes from one unit cell to another. The mechanical loading is an extension in direction 1 whatever the considered unit cell. The extension in direction 1 is associated with transverse contractions in directions 2 and 3, with a constant ratio of 0.3 between extension in direction 1 and the transverse contractions.
The layer 1 (Figure 3), whose normal is collinear to the direction of extension, is chosen as a reference layer. Its thickness, h^1, is imposed to be the same for every unit cell, in order to compare several microstructures with constant matrix volume fraction c while the particle size

L changes. The thicknesses of layers 2 and 3, supposed to be equal, are calculated to satisfy the imposed conditions (h^1, c, L) specific to each case. Projected areas A^α are evaluated in order to respect the compatibility assumption (2).
Identical extension loading in direction 1 is applied to each unit cell. We try to establish a link between the imposed macroscopic axial strain when the reference layer debonds, and the particle size. Figure 4 represents for each periodic cell the homogenized axial stress S_{11} normalized by the maximal axial stress S_{max}, vs. the imposed macroscopic strain E_{11}, normalized by the macroscopic strain E_{debond} corresponding to the first cell which undergoes a debonding of the reference layer.

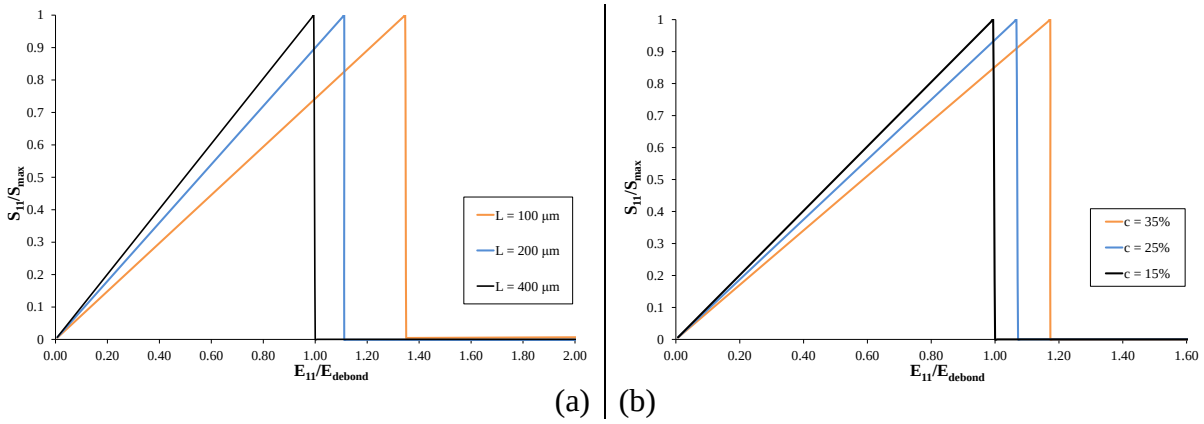

Figure 4. (a) Particle size effect on periodic cells - matrix volume fraction c = 25% - thickness of the reference layer h^1 = 10 µm, and (b) interaction effect between particles on periodic cells - particle size L = 400 µm - thickness of the reference layer h^1 = 20 µm

In Figure 4.a, results are presented for a periodic cell with 25% of matrix volume fraction and a thickness of the reference layer h^1 = 10 µm, considering three different particle sizes (L = 100 µm, 200 µm, 400 µm). We notice that the reference layer first debonds on the cell constituted of a particle of 400 µm, then a particle of 200 µm and finally a particle of 100 µm. Consequently, we notice the particle size effect experimentally observed, see e.g. Rae et al. [6]. This phenomenon was also highlighted in theoretical studies [10,11].

3.1.2. Interaction between particles

In order to observe the interaction effect between particles on periodic cells, the same type of study has been performed while fixing the particle size and changing the matrix volume fraction from one cell to another. Each generated microstructure is loaded with a uniaxial extension in direction 1. As it was done before (see 3.1.1), the damage parameters (d_{crit}, λ) and the thickness h^1 of the reference layer remain the same whatever the considered periodic cell. Every morphological parameter is evaluated following the same methodology as in 3.1.1.
Figure 4.b shows results obtained for a periodic cell with a particle size L = 400 µm and a thickness of the reference layer h^1 = 20 µm, for three different matrix volume fractions (c = 15%, 25%, 35%). Once again, an order can be seen regarding the macroscopic strains corresponding to the debonding of the reference interface of the periodic cells. Damage occurs preferentially for matrix volume fraction of 15%, then 25% and finally 35%. This confirms the crucial role of particle interactions on interfacial damage.
These first results confirm what was noticed by Inglis et al. [7] or Matouš et al. [12]: debonding occurs preferentially on large particles (particle size effect) and the stronger interactions between particles, the earlier the debonding.

3.2. Evaluation on random monomodal microstructures numerically generated

Here, we consider the responses to uniaxial extension loadings applied on artificial random monomodal microstructures. Having a high volume fraction of randomly distributed particles, these microstructures present a more consistent morphology with real materials than previous periodic cells. . The volumes of particles are moderately scattered around an average value, chosen to be the volume of a spherical particle of diameter L. The constituents have a linear elastic behavior [3] as in Section 3.1. Whatever the studied microstructure, the same uniaxial extension loading is applied and each configuration is characterized by the same damage parameters (d_{crit}, λ).
We try to establish a link between the macroscopic axial strains corresponding to the moment when the first debonding occurs and particle size or matrix volume fraction. Many computations are performed on random samples of this type of microstructure, and macroscopic axial strains corresponding to the first nucleation are statistically analyzed [13,14]. Three different matrix volume fractions c and three average particle sizes L are considered: nine configurations (c, L) are studied. Ten realizations are generated for each configuration.

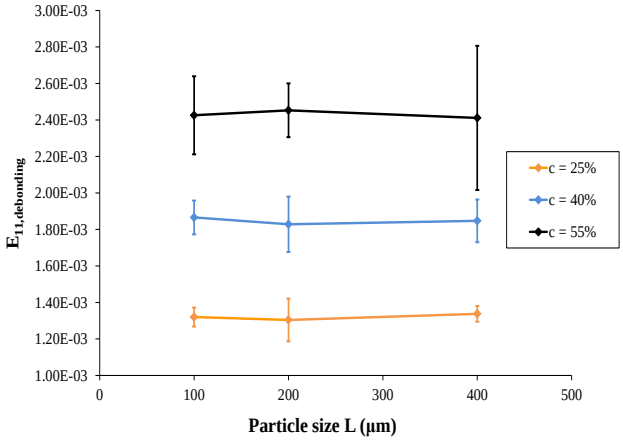

Figure 5. Particle size effect and interaction between particles on random monomodal microstructures - c is the matrix volume fraction, $E_{11,debonding}$ the macroscopic strain of first debonding into the microstructure.

Considering a constant particle size (Figure 5), it is possible to observe that the most important the particle volume fraction, the earlier the first nucleation. This result was highlighted by [7,12] through full-field simulations. Moreover, it can be seen that the amplitude of the variation intervals around the average decreases when the matrix volume fraction decreases (i.e. when the particle volume fraction increases). This observation illustrates the efficiency of the M.A. better adapted to high particle volume fractions than the Mori-Tanaka scheme used by Tan et al. [10,15] and evaluated in [7].
Considering a constant matrix volume fraction and an evolutive particle size (Figure 5), any significant trend of the average macroscopic strain corresponding to the first debonding can be detected. In other words, no particle size effect may be evidenced for the studied microstructures. This may be attributed to their monomodal character that endows them a certain similarity.

3.3. Evaluation on a random bimodal microstructure numerically generated

A random bimodal microstructure numerically generated is here tested. The volumes of particles present two majority average values, which define the domain of “small particles”

and the domain of "large particles". Then, the nucleation chronology in this microstructure has been studied for to evaluate the M.A. ability to deal with particle size effects.
The studied microstructure contains more than 7000 particles (volume fraction: 76% - Figure 6). While keeping the same mechanical properties for the constituents and the same damage parameters (d_{crit}, λ), nine uniaxial extensions in different directions are applied on our random bimodal microstructure, for a statistical analysis of the nucleation chronology with respect to the orientation effects.
Results are illustrated in Figure 6. The granulometric repartition of the microstructure is superposed to points characterizing interfacial nucleations: the graph presents the macroscopic strain corresponding to interfacial debonding vs. volume of particle. First debondings occur for "large particles". Then, damage appears for some "small particles", while the phenomenon continues to come forward on "large particles". From a general statistical viewpoint, we have observed that the most important the macroscopic strain, the more "small particles" debond. Consequently, these results show an influence of particle size.

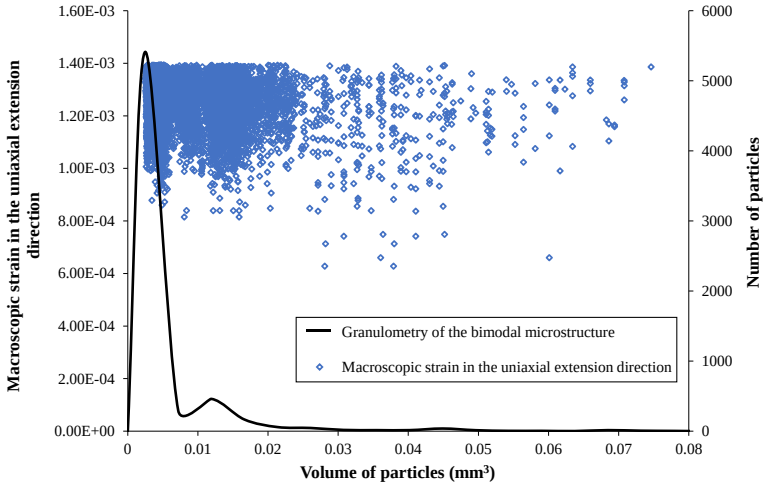

Figure 6. Granulometric repartition of the random bimodal microstructure and influence of particle size on debonding chronology.

4. Conclusions

Through this work, the predictive abilities of the M.A. in the small strain framework have been evaluated. Only one non-linearity is considered: interface debonding [3].
The particle size effect was observed on simple periodic microstructures and on a random bimodal microstructure. It allowed us to confirm the observations made in literature [6].
On the other hand, results show the capacities of the M.A. to take into account the complex interaction effects between the grains due to high particle volume fraction, thanks to the description of the field heterogeneity into the matrix as a function of the morphology of the intergranular zone, unlike the mean-field methods [7].

Funding acknowledgements

This study is financially supported by Direction Générale pour l'Armement and Région Poitou-Charentes through Marion Trombini's PhD grant.

References

[1] L. R. Cornwell and R. A. Schapery. SEM study of microcracking in strained solid propellant . *Metallography*, vol. 8: pp. 445–452, 1975.

[2] C. Nadot-Martin, M. Touboul, A. Dragon, and A. Fanget. Direct scale transition approach for highly-filled viscohyperelastic particulate composites: computational study . In O. Cazacu, Ed., *Multiscale modeling of heterogeneous materials: from microstructure to macro-scale properties*, pp. 218–237. *ISTE/Wiley*, 2008.

[3] S. Dartois, C. Nadot-Martin, D. Halm, A. Dragon, A. Fanget, and G. Contesse. Micromechanical modelling of damage evolution in highly filled particulate composites - Induced effects at different scales . *Int. J. Damage Mech.*, (DOI: 10.1177/1056789512468916): , 2013.

[4] E. Kimura and Y. Oyumi. Shock ignitability test for azide polymer propellants . *J. Energ. Mater.*, vol. 16: pp. 173–185, 1998.

[5] T. Naya and M. Kohga. Influences of particle size and content of HMX on burning characteristics of HMX-based propellant . *Aerosp. Sci. Technol.*, vol. 27 (1): pp. 209–215, 2013.

[6] P. J. Rae, S. J. P. Palmer, H. T. Goldrein, J. E. Field, and A. L. Lewis. Quasi-static studies of the deformation and failure of PBX 9501 . *Proc. R. Soc. A Math. Phys. Eng. Sci.*, vol. 458 (2025): pp. 2227–2242, 2002.

[7] H. M. Inglis, P. H. Geubelle, K. Matous, H. Tan, and Y. Huang. Cohesive modeling of dewetting in particulate composites: micromechanics vs. multiscale finite element analysis . *Mech. Mater.*, vol. 39 (6): pp. 580–595, 2007.

[8] J. Christoffersen. Bonded granulates . *J. Mech. Phys. Solids*, vol. 31 (1): pp. 55–83, 1983.

[9] C. Nadot, A. Dragon, H. Trumel, and A. Fanget. Damage modelling framework for viscoelastic particulate composites via a scale transition approach . *J. Theor. Appl. Mech.*, vol. 44: pp. 553–583, 2006.

[10] H. Tan, Y. Huang, C. Liu, and P. H. Geubelle. The Mori–Tanaka method for composite materials with nonlinear interface debonding . *Int. J. Plast.*, vol. 21 (10): pp. 1890–1918, 2005.

[11] C. B. Ma, H. F. Qiang, W. M. Wu, and J. Xue. Microstructure and damage analysis of solid propellant . *Adv. Heterog. Mater. Mech.*, pp. 218–221, 2011.

[12] K. Matous, H. M. Inglis, X. Gu, D. Rypl, T. L. Jackson, and P. H. Geubelle. Multiscale modeling of solid propellants: from particle packing to failure . *Compos. Sci. Technol.*, vol. 67: pp. 1694–1708, 2007.

[13] T. Kanit, S. Forest, I. Galliet, V. Mounoury, and D. Jeulin. Determination of the size of the representative volume element for random composites: statistical and numerical approach . *Int. J. Solids Struct.*, vol. 40 (13)–(14): pp. 3647–3679, 2003.

[14] T. Kanit, F. N'Guyen, S. Forest, D. Jeulin, M. Reed, and S. Singleton. Apparent and effective physical properties of heterogeneous materials: Representativity of samples of two materials from food industry . *Comput. Methods Appl. Mech. Eng.*, vol. 195 (33)–(36): pp. 3960–3982, 2006.

[15] H. Tan, C. Liu, Y. Huang, and P. Geubelle. The cohesive law for the particle/matrix interfaces in high explosives . *J. Mech. Phys. Solids*, vol. 53 (8): pp. 1892–1917, 2005.